



HEAT AND MASS TRANSFER EFFECTS ON CONVECTIVE MHD SLIP FLOW WITH VARIABLE VISCOSITY OVER INCLINED POROUS MEDIUM

S. A. Amoo¹, Akeem B. Disu², & A. S. Idowu³

¹Department of Mathematics and Statistics, Federal University
Wukari, Wukari, Nigeria

²Department of Mathematics, National Open University of Nigeria

³Department of Mathematics, University of Ilorin, Ilorin, Nigeria
drsikiruamoo@gmail.com, adisu@noun.edu.ng, asidowu@gmail.com

ABSTRACT

The study investigated effects of heat and mass transfer on convective Magnetohydrodynamics (MHD) slip flow over an inclined porous medium in the presence of variable viscosity and heat generations. The governing boundary layer equations of the model were transformed to a system of ordinary coupled differential equations. The coupled system of nonlinear equations were solved numerically using a fourth order Runge-Kutta method and method of shooting technique. A parametric study on the effect of variations of the radiation, magnetic, thermal conductivity grashof number, solutal grashof, pranddtl, schmidt, chemical species parameters and angle of inclination at the surface on velocity, temperature and concentration were presented graphically. Also, the effects of these parameters were presented numerically for skin friction, Nusselt and Sherwood numbers.

Keywords: MHD slip flow, Variable viscosity, Inclined surface, Chemical Reaction, Porous Media

INTRODUCTION

Heat flow over a moving stretching surface has important applications in electrochemistry and polymer processing. For example, (i) materials manufactured by extrusion processes and heat treated materials travelling between a feed roll and a windup roll or on a conveyor belt possess the characteristics of a moving stretching surface (Devi, Neeraj, and Reddy (2015)) and (ii) metallurgical processes involve the cooling of continuous strips or filaments by drawing them through a quiescent fluid and that in the process of drawing, these strips are sometimes stretched.

In view of the applications of the moving stretching surface, Mukhopadhyay (2012) investigated the slip effect on MHD boundary layer over exponentially stretching sheet. Mukhopadhyay and Gorla (2008) presented the effects of partial slip on boundary layer flow past a permeable exponentially stretching sheet in the presence of thermal radiation, heat and mass transfer. Shekhar (2014) carried out analysis on the

boundary layer phenomena of MHD flow and heat transfer over an exponentially stretching sheet embedded in a thermally stratified medium. The researchers neglected the chemical reaction.

Ibrahim and Suneetha (2015) studied the effects of heat generation and thermal radiation on steady MHD flow near a stagnation point on a stretching sheet in porous medium and presence of variable thermal conductivity and mass transfer. Devi, Neeraj, and Reddy (2015) investigated radiation effect on MHD slip flow past a stretching sheet with variable viscosity and heat source/sink. Amoo, Babayo and Amoo (2017) considered nonlinear MHD boundary layer flow embedded in Darcy-Forchheimer Porous Medium with Viscous dissipation and Chemical Reaction. All these studies are horizontally stretching surface.

However, the study of heat transfer through a porous medium is important, because of its applications in soil mechanics, water purification, underground water hydrology,

chemical engineering,
petroleum engineering,
ceramic engineering,
metallurgical engineering,
agricultural engineering and
water irrigation process (Disu
and Dada (2017)).

Despite the application of fluid flow through a porous medium, the study of the combination of heat and mass transfer effects using radiation and chemical reaction with MHD slip flow has drawn attention of few researchers (Amoo and Idowu (2017)).

In view of the above studies, the present study investigated effects of heat and mass transfer on convective Magnetohydrodynamics (MHD) slip flow over inclined porous media in the presence

of variable viscosity and heat generation.

Mathematical Analysis

Consider the heat and mass transfer of a two-dimensional MHD slip flow over an inclined porous medium in the present of radiation (**Figure 1**). A uniform transverse magnetic field $B(x)$ is applied perpendicular to the direction of the fluid flow. The flow is assumed to be in the x - direction with y -axis normal to it. The plate is maintained at the temperature and species concentration T_w , C_w and free stream temperature and species concentration T_∞ , C_∞ respectively, while α is the angle of inclination. The equations governing the fluid flow are as follows:

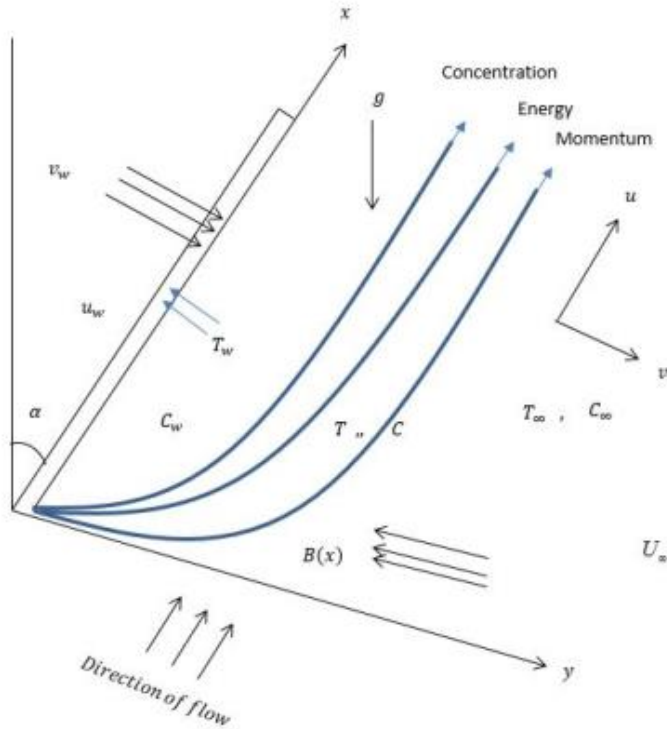


Figure 1: The physical model and coordinate system

$$\frac{\partial u}{\partial x} + \frac{\partial v}{\partial y} = 0$$

(1)

$$u \frac{\partial C}{\partial x} + v \frac{\partial C}{\partial y} = D \frac{\partial^2 C}{\partial y^2} - \gamma(C - C_\infty)$$

$$u \frac{\partial u}{\partial x} + v \frac{\partial u}{\partial y} = \frac{1}{\rho} \frac{\partial \mu}{\partial T} \frac{\partial T}{\partial y} \frac{\partial u}{\partial y} + \frac{\mu}{\rho} \frac{\partial^2 u}{\partial y^2} - \frac{1}{\rho} \sigma B^2(x) u + g \beta_T (T - T_\infty) \cos(\alpha) + g \beta_C (C - C_\infty) \cos(\alpha)$$

(2)

Subject to the following boundary conditions:

$$\rho C_p \left(u \frac{\partial T}{\partial x} + v \frac{\partial T}{\partial y} \right) = k \frac{\partial^2 T}{\partial y^2} - \frac{\partial q_r}{\partial y} + Q_0 (T - T_\infty)$$

(3)

$$u = U_0 e^{\frac{x}{L}}, v = -V_0 e^{\frac{x}{L}}, T = T_w = T_x + T_0 e^{\frac{x}{L}}, C = C_w = C_x + C_0 e^{\frac{x}{L}} \text{ at } y=0$$

$$u \rightarrow 0, T \rightarrow T_\infty, C \rightarrow C_\infty \text{ as } y \rightarrow \infty$$

(5)

where u , v , C , and T are velocity component in the x direction, velocity component

in the y direction, concentration of the fluid species and fluid temperature respectively. L is the reference length, $B(x)$ is the magnetic field strength, U_0 is the reference velocity and V_0 is the permeability of the porous surface. The physical parameters K , ρ , ν , σ , D , k , C_p , Q_0 and γ are the permeability of the porous medium, density, fluid kinematics viscosity, electric conductivity of the fluid, coefficient of mass diffusivity, thermal conductivity of the fluid, specific heat, rate of specific internal heat generation or absorption and reaction rate coefficient respectively. g is the gravitational acceleration, β_T and β_C are the thermal and mass expansion coefficients respectively and q_r is the radiative heat flux in the y direction.

Introducing the stream function $\psi(x, y)$ such that

By using the Rosseland approximation according to Ibrahim and Suneetha (2015). The radiative heat flux q_r is given by

$$q_r = -\frac{4\sigma_0}{3\delta} \frac{\partial T^4}{\partial y}$$

(6)

where σ_0 and δ are the Stefan-Boltzmann and the mean absorption coefficient respectively. Assume the temperature difference within the flow are sufficiently small such that T^4 may be expressed as a linear function of temperature, using Taylor series to expand T^4 about the free stream T_∞ and neglecting higher order terms, this gives the approximation

$$T^4 \cong 4T_\infty^3 T - 3T_\infty^4 \quad (7)$$

The magnetic field $B(x)$ is assumed to be in the form

$$B(x) = B_0 e^{\frac{x}{2L}} \quad (8)$$

where B_0 is the constant magnetic field.

$$u = \frac{\partial \psi}{\partial y}, \quad v = -\frac{\partial \psi}{\partial x} \quad (9)$$

Temperature dependent viscosity according to Devi, *et al.* (2015) is of the form:

$$\mu = \mu_1 a + b(T_w - T) \quad (10)$$

Where μ_1 is the constant value of the coefficient of viscosity in the free stream and a, b are constants with $b(> 0)$ having unit K^{-1} . Here viscosity temperature relation $\mu = a_1 - b_1 T$ which accords the relation $\mu = e^{-a_1 T}$ when second and higher order terms are neglected.

Temperature dependent viscosity according to Devi, *et al.* (2015) is of the form:

$$\mu = \mu_1 a + b(T_w - T) \quad (10)$$

Where μ_1 is the constant value of the coefficient of viscosity in the free stream and a, b are constants with $b(> 0)$ having unit K^{-1} . Here viscosity temperature relation $\mu = a_1 - b_1 T$ which accords the relation $\mu = e^{-a_1 T}$ when second and higher order terms are neglected from the expansion. The expression of kinematic viscosity becomes

$$\nu = \nu_1 a + b(T_w - T) \quad , \quad \text{where}$$

$$\nu_1 = \frac{\mu_1}{\rho} \quad \text{the constant value of}$$

the kinematic fluid viscosity. Substituting (9) in (1), continuity equation satisfied Chauchy-Riemann equation and equations (2)-(4), give

$$\frac{\partial \psi}{\partial y} \frac{\partial T}{\partial x} - \frac{\partial \psi}{\partial x} \frac{\partial T}{\partial y} = \left(\frac{k}{\rho C_p} + \frac{16\sigma_0 T_\infty^3}{3\rho C_p \delta} \right) \frac{\partial^2 T}{\partial y^2} + \frac{Q_0}{\rho C_p} (T - T_\infty) \quad (12)$$

$$\frac{\partial \psi}{\partial y} \frac{\partial C}{\partial x} - \frac{\partial \psi}{\partial x} \frac{\partial C}{\partial y} = D \frac{\partial^2 C}{\partial y^2} - \gamma(C - C_\infty) \quad (13)$$

The corresponding boundary conditions become:

$$\begin{aligned} \frac{\partial \psi}{\partial y} &= U_0 e^{\frac{x}{L}} = cx + L \frac{\partial u}{\partial y}, \quad \frac{\partial \psi}{\partial x} = V_0 e^{\frac{x}{L}}, \quad T = T_w = T_\infty + T_0 e^{\frac{x}{L}}, \\ C &= C_w = C_\infty + C_0 e^{\frac{x}{L}} \quad \text{at } y = 0 \\ \frac{\partial \psi}{\partial y} &\rightarrow 0, T \rightarrow T_\infty, C \rightarrow C_\infty \quad \text{as } y \rightarrow \infty \end{aligned} \quad (14)$$

In order to transform the equations (11), (12) and (13) as well as the boundary conditions (14) into an ordinary differential equations, the following similarity transformations variables are introduced following Sajid and Hayat (2008).

$$\psi(x, y) = \sqrt{2\nu U_0} L e^{\frac{x}{2L}} f(\eta), \eta = y \sqrt{\frac{U_0}{2\nu L}} e^{\frac{x}{2L}}, T = T_\infty + T_0 e^{\frac{x}{2L}} \theta(\eta),$$

$$C = C_\infty + C_0 e^{\frac{x}{2L}} \phi(\eta)$$

(15)

The equation becomes

$$(a + A - A\theta)f''' + ff'' - A\theta f' - f'^2 - Mf' + G_r \theta \cos(\alpha) + G_c \phi \cos(\alpha) = 0$$

(16)

$$\left(1 + \frac{4}{3}R\right)\theta'' + P_r f \theta' - P_r f' \theta + P_r Q \theta = 0$$

(17)

$$\phi'' + S_c f \phi' - S_c f' \phi - S_c \lambda \phi = 0$$

(18)

The corresponding boundary conditions take the form:

$$f = f_w, f' = 1 + \delta f'', \theta = 1, \phi = 1 \text{ at } \eta = 0,$$

$$f' = 0, \theta = 0, \phi = 0 \text{ as } \eta \rightarrow \infty$$

(19)

where $\delta = L \left(\frac{C}{\nu_1}\right)^{\frac{1}{2}}$ is the slip parameter, $A = b(T_w - T)$ is the viscosity parameter,

$M = \frac{2\sigma L B_0}{\rho U_0} e^{\frac{x}{2L}}$ is the magnetic parameter,

$G_c = \frac{2Lg\beta_r T_0}{U_0^2} e^{\frac{3x}{2L}}$ is the thermal Grashof number,

$G_c = \frac{2Lg\beta_c C_0}{U_0^2} e^{\frac{3x}{2L}}$ is the solutal Grashof number,

$Pr = \frac{\rho\nu C_p}{k} = \frac{\mu_1 c_p}{k}$ is the Prandtl number, $R = \frac{4\sigma_0 T_\infty^3}{3k}$ is the radiation parameter, $Q = \frac{2LQ_0}{U_0 \rho C_p} e^{-\frac{x}{L}}$ is the heat generation parameter, while α is the angle of inclination, $Sc = \frac{\nu_1}{D}$ is the Schmidt number, $\lambda = \frac{2L\gamma}{U_0} e^{-\frac{x}{L}}$ is the chemical reaction parameter, $f_w = V_0 \sqrt{\frac{2L}{\nu U_0}} e^{-\frac{3x}{2L}}$ is the permeability of the plate.

The skin friction coefficient was written as

$C_f \left(\frac{Re_x}{2}\right)^{\frac{1}{2}} = f''(0)$, the local Nusselt number was written as

$Nu \left(\frac{Re_x}{2}\right)^{\frac{1}{2}} = -\theta'(0)$ and the local Sherwood number stood as

$Sh \left(\frac{Re_x}{2}\right)^{\frac{1}{2}} = -\phi'(0)$

The equations (16), (17) and (18) are highly non-linear coupled differential equations and its satisfying the boundary conditions (19). The problem being a boundary value problem, applying a shooting technique (guessing the unknown values) to change the conditions to initial value problem. Equations (16-18) along with the boundary conditions (19) were solved numerically by applying Nachtsheim-Swigert shooting iteration technique along with Runge-Kutta fourth-order integration scheme. The computations were performed using a symbolic program and computational computer language Maple 18. The step size is taken to be $\Delta\eta = 0.001$ to satisfy the relative convergence requirement of 10^{-5} in all cases. The value of

η_{∞} is noticed to the iteration loop by $\eta_{\infty} = \eta_{\infty} + \Delta\eta$. The highest value of η_{∞} to each parameter was determined when the values of the unknown boundary conditions at $\eta = 0$ did not change after successful loop with error less than 10^{-5} .

Results

The process of numerical computation showed the skin-friction coefficient, the local Nusselt number and the local Sherwood number, which were respectively proportional to $f''(0)$, $\theta'(0)$ and $\phi'(0)$, at the plate were examined for different values of the parameters. The comparison of the present study with the skin friction of the existing works are presented in Table 1 for values of δ when $A=0$.

Values	Present study	Devi et al (2015)	Bhattacharyya and Layek (2010).
Values	$f''(0)$	$f''(0)$	$f''(0)$
0.0	-0.000000	-1.000480	-1.000000
0.1	-0.876889	-0.872571	-0.872083
0.2	-0.788871	-0.776867	-0.776377
0.5	-0.646494	-0.591683	-0.591105

Table 1 shows numerical values of skin friction when compared with the existing literature and were in close agreement. The present study shows improvement over the previous studies. In our computation, we set the flow parameters as: $a = 0.33$, $A = 0.21$, $\lambda = 0.50$, $Gr = 1$, $Gc = 0.01$, $Q = 0.5$, $M = 0.001$, $f_w = 1$, $R = 1$, $Sc = 0.35$, $\alpha = 5^0$, $Ec = 0.05$, $Pr = 0.72$. All graphs correspond to the value except otherwise indicated on the graph.

Table 2: Effect of f_w , G_r , G_c , S_c , P_r , and R on $f''(0)$, $\theta'(0)$ and $\phi'(0)$ (P-Parameters)

P	Valu	$f''(0)$	$-\theta'(0)$	$-\phi'(0)$	P	Valu	$f''(0)$	$-\theta'(0)$	$-\phi'(0)$	
a	0.33	15.09	-	1.932	A	2.1	9.096	-	1.863	
		80	1.295	39			95	1.243	92	
			25					09		
	0.35	14.22	-	1.927	2.2	2.2	9.502	-	1.867	
		11	1.286	02			30	1.253	34	
			65					26		
	0.37	13.43	-	1.921	2.3	2.3	9.903	-	1.870	
		90	1.277	69			10	1.262	31	
			94					04		
	0.39	12.73	-	1.916	2.5	2.5	10.69	-	1.875	
		67	1.269	43			06	1.276	19	
			12					21		
M	0.00	0.014	0.698	0.681	S	0.35	5.628	-	1.306	
		1	12	31			00	26	1.162	61
									82	
	2.0	0.274	-	0.722	0.62	0.62	4.829	-	1.785	
		22	0.051	71			78	0.961	69	
			78					09		
	3.0	0.352	-	0.742	1.50	1.50	4.031	-	3.022	
		90	0.633	26			47	0.783	27	
			42					11		
	4.0	0.419	-	0.764	2.00	2.00	3.845	-	3.641	
		63	1.449	82			34	0.750	45	
			56					63		

G_r	1.0	0.096 98	0.555 88	0.691 98	P_r ,	0.72	4.829 78	- 0.961 09	1.785 67
	2.0	0.494 15	0.527 75	0.715 55		0.78	5.107 41	- 1.062 32	1.793 54
	3.0	0.899 35	0.492 61	0.738 09		0.84	5.407 64	- 1.164 52	1.801 42
	4.0	1.753 95	0.400 82	0.781 81		0.90	5.732 59	- 1.268 08	1.809 31
G_c	0.01	- 0.206 69	0.436 16	0.677 22	R	0.5	4.829 78	- 0.961 09	1.785 67
	3.10	0.942 07	0.258 34	0.747 06		1.7	3.539 48	- 0.355 74	1.736 92
	3.80	1.199 33	0.214 62	0.760 03		4.7	2.991 67	0.011 82	1.704 96
	5.00	1.641 84	0.138 30	0.780 78		7.0	2.880 26	0.097 88	1.697 12
f_w	1.00	4.829 78	- 0.961 09	1.785 67	Q	0.5	4.829 78	- 0.961 09	1.785 67
	2.00	3.318 37	- 0.036 57	2.106 85		0.8	5.643 74	- 1.261 35	1.815 37
	3.00	2.114 75	0.759 20	2.509 62		1.0	6.292 97	- 1.474 92	1.836 22
	4.00	1.280 80	1.405 52	2.982 73		1.5	8.310 82	- 2.050 80	1.889 44
λ	0.5	4.829 78	- 0.961 09	1.785 67	α	5 ⁰	- 0.488 14	0.420 69	0.652 72

	1.5	4.695	-	1.963	8^0	-	0.408	0.618	
		44	0.930	59		0.895	96	14	
			43			44			
	2.5	4.585	-	2.127	11^0	-	0.415	0.631	
		68	0.905	36		0.747	26	45	
			75			98			
	4.0	4.453	-	2.352	14^0	-	0.418	0.641	
		26	0.876	25		0.622	64	99	
			56			91			
<i>E</i>	0.05	1.926	0.956	1.613	<i>E</i>	0.55	6.116	-	1.832
<i>c</i>		10	75	44	<i>c</i>		30	1.433	12
							13		
	0.50	4.829	-	1.785	0.57	6.770	-	1.851	
		78	0.961	67		36	1.641	82	
			09				47		

DISCUSSION

Table 2 represents the numerical results of variation in Skin friction, Nusselt and Sherwood numbers at the surface with a , A , M , Gr , Gc , f_w , Q , Sc , Pr , R , α and λ which are of physical and engineering interest. It could be observed from the results that an increase in the values of a , A , M , f_w , Sc and Pr decreased the flow boundary layer while increase in M , Gc , Gr , Ec , Q and R increase the flow boundary layer. R , Sc , Q Ec , and a decreased thermal boundary layer. The table depicts that an increase in the values of M , Q , Gr , Gc , and R thicken the thermal boundary

layer by reducing the rate at which heat diffuse out of the system while increase in f_w , Sc , λ and Pr reduce the thickness of the thermal boundary layer. Also, the results showed that increase in Pr , causes thinning in the concentration boundary layer while M , R , Gr , Gc , Sc , Q , f_w , and λ thicken the mass boundary layer. Graphical interpretation of relevant parameters were equally presented in figures 2-14. Figure 2 showed the effect of slip conditions on the velocity, temperature and concentration profiles. The dimensionless parameter describing the slip condition at $a = 0$, suggest no

slip condition in the fluid flow. As we increased the parameter, it was discovered that the rate of flow decreased as well as thermal and concentration boundary layers too. Figure 3 illustrated the effects of A parameter on the rate of flow. It was discovered that as the parameter A increased, rate of flow increased as well as concentration profile with corresponding decreased in the thermal boundary layer. Figure 4 explained the effect of magnetic parameter M on the fluid flow. The effect of increased M led to the corresponding increase in skin friction, and Sherwood number but decreased the Nusselt number or thermal boundary layer. The implication of this transport of fluid flow was that when magnetic field strength was applied transversely to the flow, it gave rise to opposing force called Lorentz force.

Figure 5 showed the effects of thermal Grashoff number on the local velocity, temperature and concentration profiles. The influence showed that as we increased Gr , there were corresponding increase in fluid flow and mass boundary layer but decrease in thermal boundary layer hence law

temperature profiles. Figure 6 depicted the effects of solutal Grashof number in the local skin friction, temperature profile and concentration. It was discovered that as we increased G_c , there was increase in skin friction and Sherwood numbers but a reverse in Nusselt number. Figure 7 illustrated effects of inclination on the MHD fluid with slip condition. It was found that increase in α led to decrease in velocity and thermal boundary layers whereas its effect led to increase in concentration profile. Figure 8 showed the effect of heat source/sink on MHD slip flow. It was discovered that Q decreased thermal boundary layer but as we increased Q , the velocity and concentration profiles of the fluid increased correspondingly. Figure 9 depicted the effect of chemical reaction on the local velocity, temperature and concentration profiles. It was shown that chemical reaction decreased the velocity profile but increased the temperature and concentration of the fluid. Figure 10 described the effect of Schmidt number Sc . On the velocity, temperature and concentration profiles. It was observed that increased Sc parameter decreased velocity

profile but increased thermal and concentration boundary layers. Figure 11 showed the effect of Prandtl number Pr on the velocity, temperature and concentration profiles respectively. The increase in Pr caused decrease in temperature profile but the same increased the velocity and concentration. It is worth mentioning that figure 12 implemented the porosity at the plate thereby showing the effects on velocity, temperature and concentration profiles. The increase in fw showed decrease in velocity profile but increased the temperature and concentration profiles. The effects of thermal radiation R on velocity, temperature and concentration profiles was depicted in figure 13. When R was increased, it enhanced the heat flux from the plate and this was able to increase the velocity and temperature profiles. However, its increase decreased the concentration profile. In figure 14 it was discovered that increase in Eckert number led to the increase velocity and concentration profile but decrease in temperature profile.

Conclusions

In this article, the steady case of MHD slip flows over inclined porous media was considered. The results obtained was compared with the existing result in literature and it was found to be in excellent agreement. The conclusions drawn from the study were:

- Increased slip condition parameter decreased velocity, temperature, time and concentration profiles
- Permeability decreased the velocity profile but increased the thermal concentration profiles
- Magnetic parameter increase both velocity and concentration profile but decreased temperature profile.
- Radiation increased both velocity and temperature profiles but not concentration profile.
- Eckert number increased both skin friction and Sherwood numbers but not solutal Grashof numbers
- Both thermal and solutal grashof numbers increased both velocity and concentration but both decreased the

thermal boundary layer or temperature profile. It was therefore remarkable to not that the study is

recommended for use in industries.

Graphs

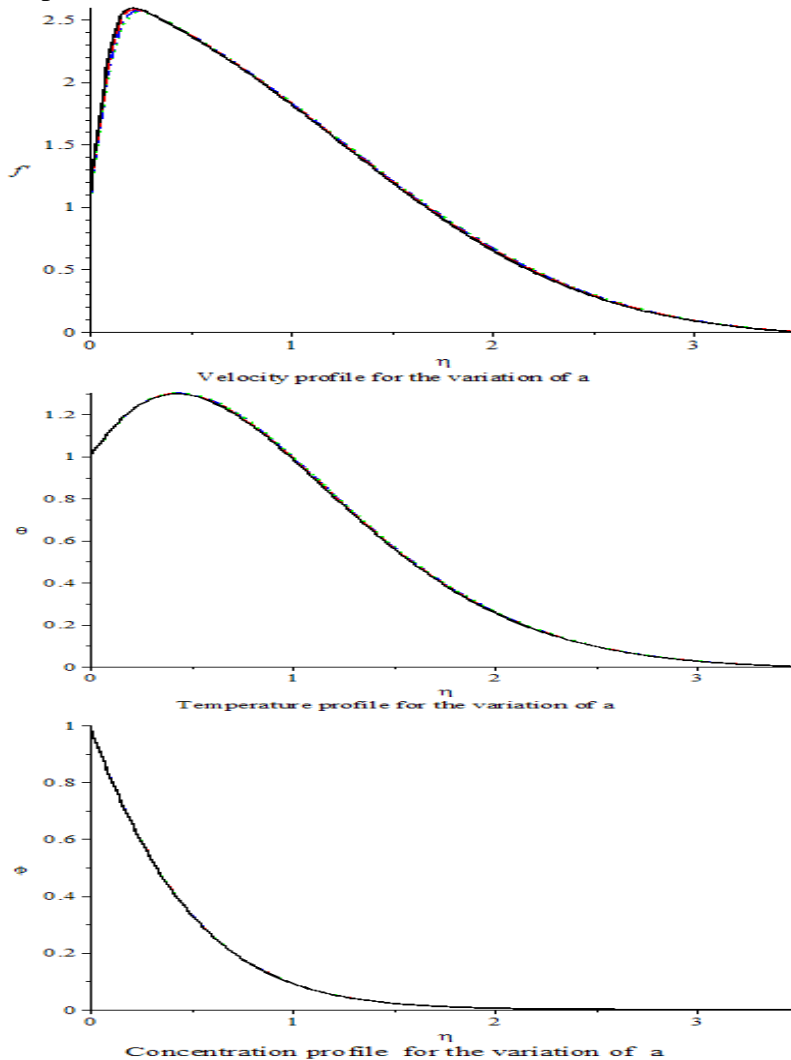
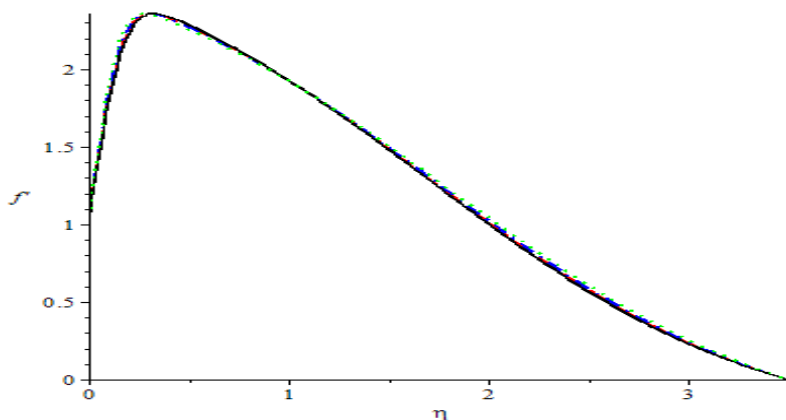
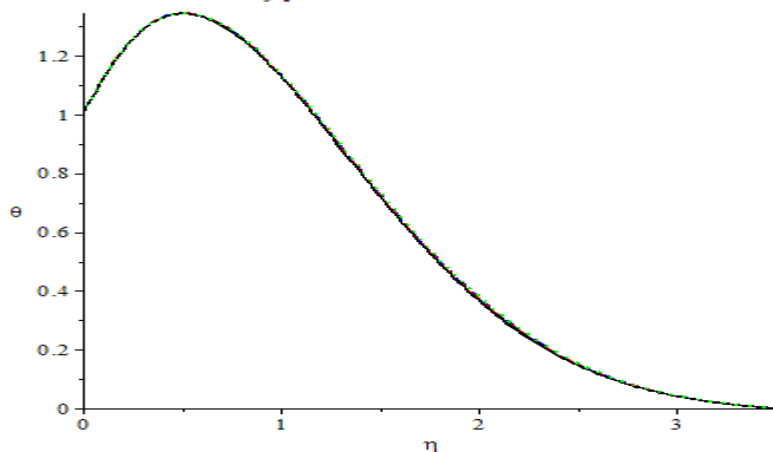


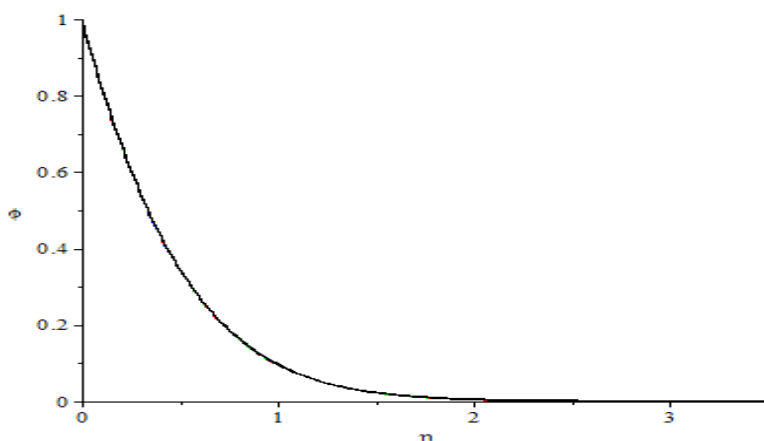
Figure 2: Effect on velocity, temperature and concentration profiles



Velocity profile for the variation of A



Temperature profile for the variation of A



Concentration profile for the variation of A

Figure 3: A effect on velocity, temperature and concentration profiles

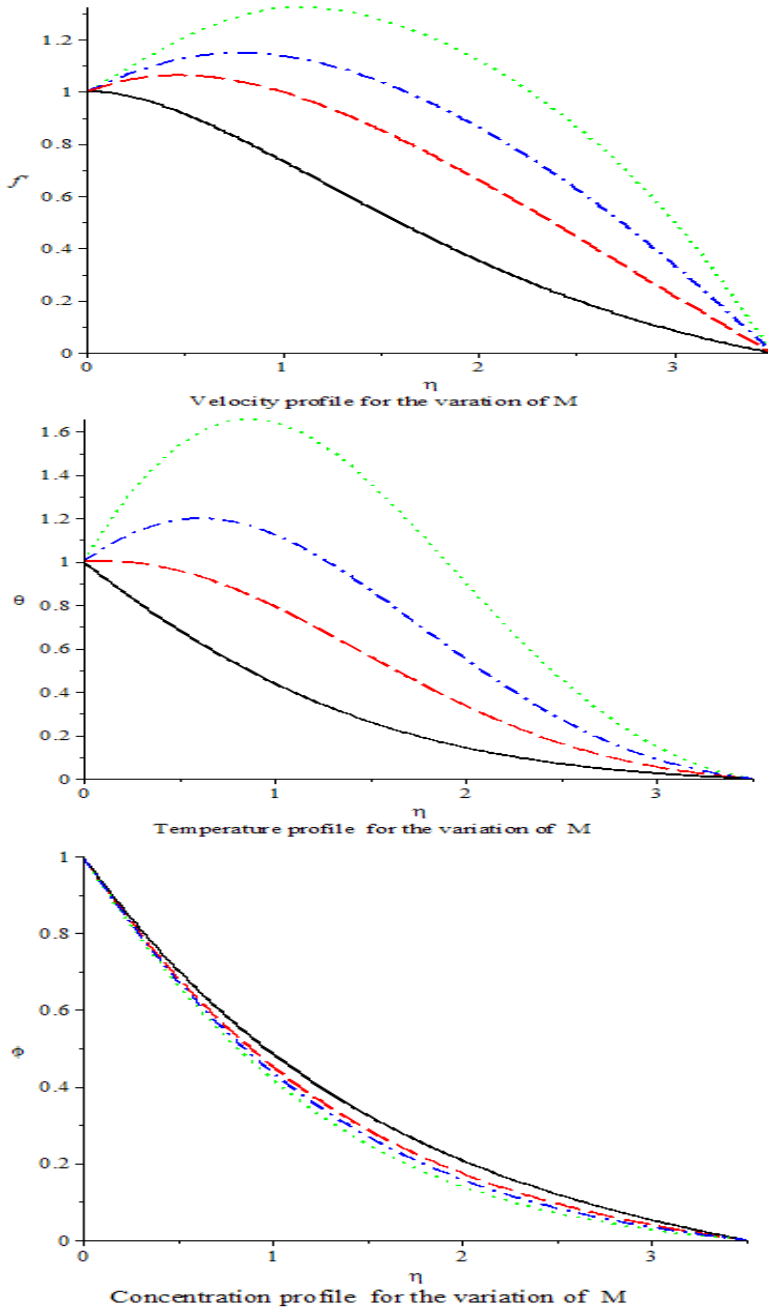


Figure 4: M effect on velocity, temperature and concentration profiles

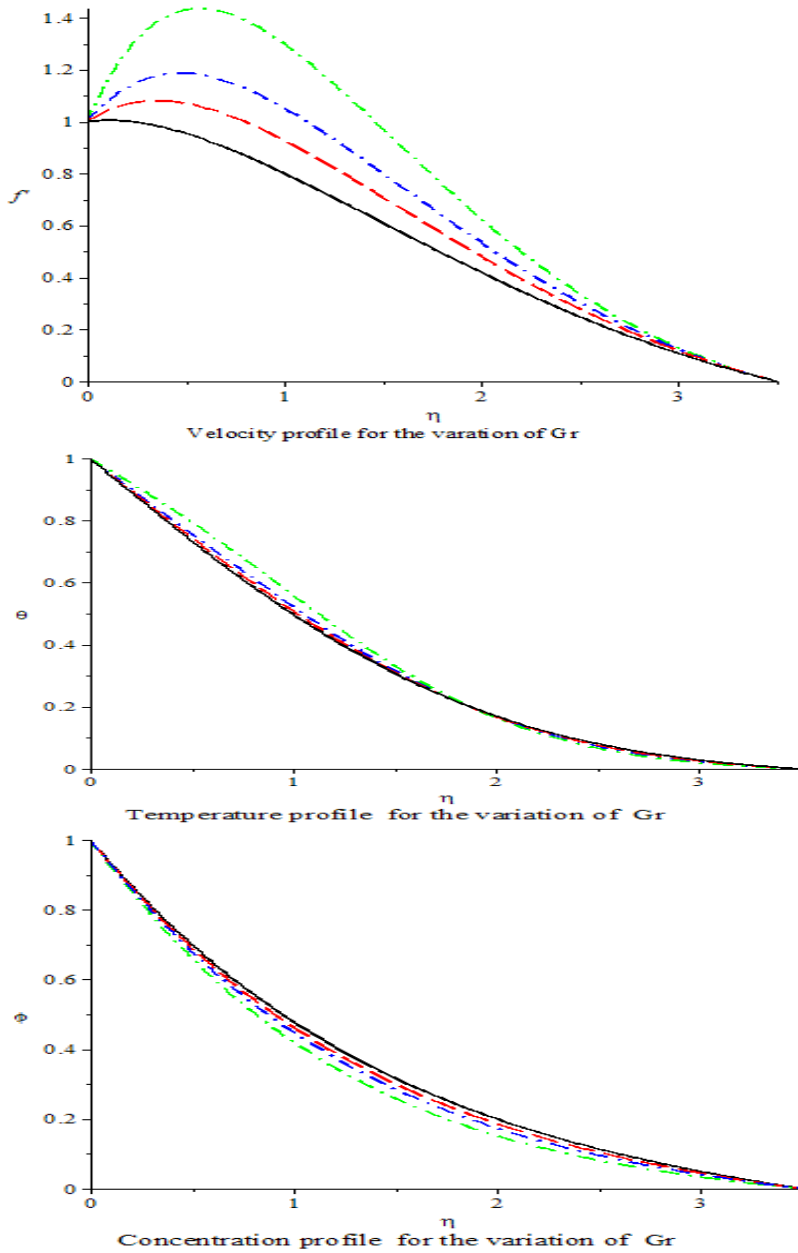


Figure 5: Gr effect on velocity, temperature and concentration profiles

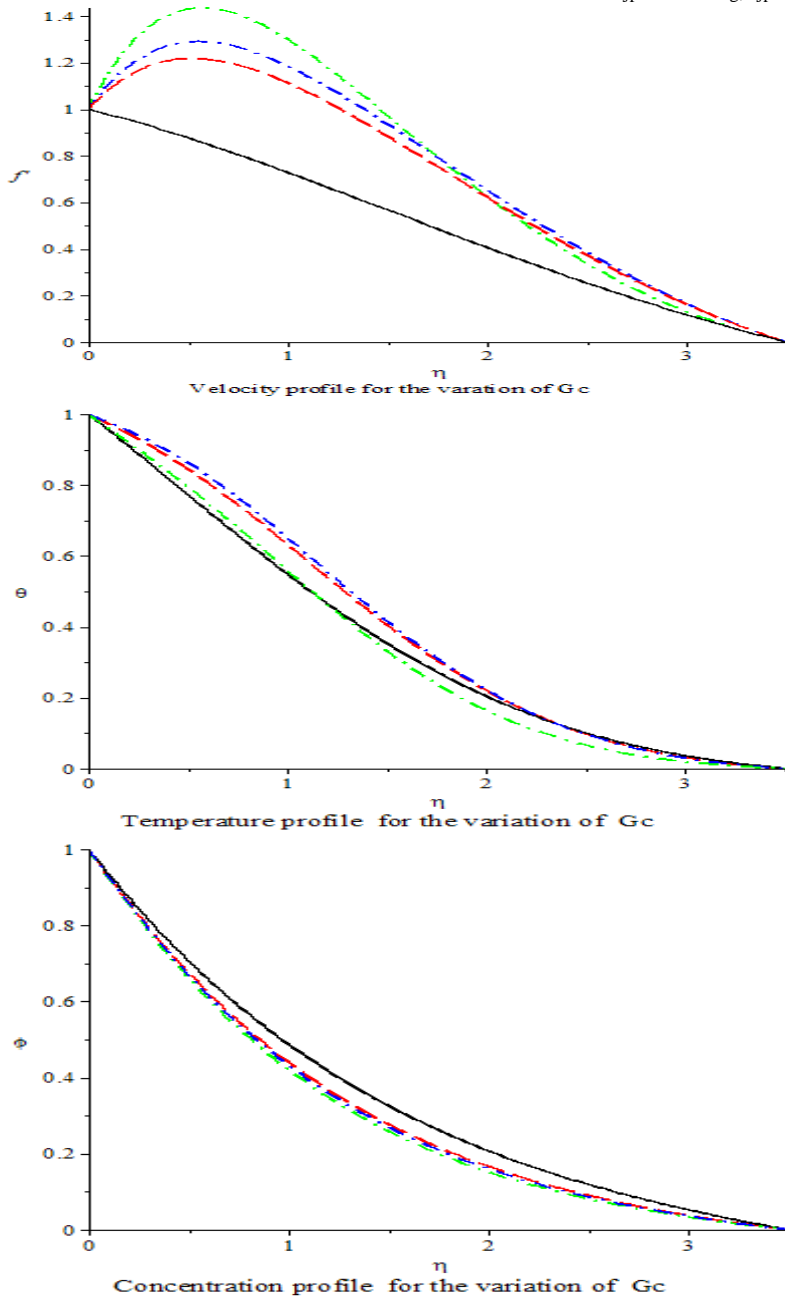


Figure 6: G_c effect on velocity, temperature and concentration profiles

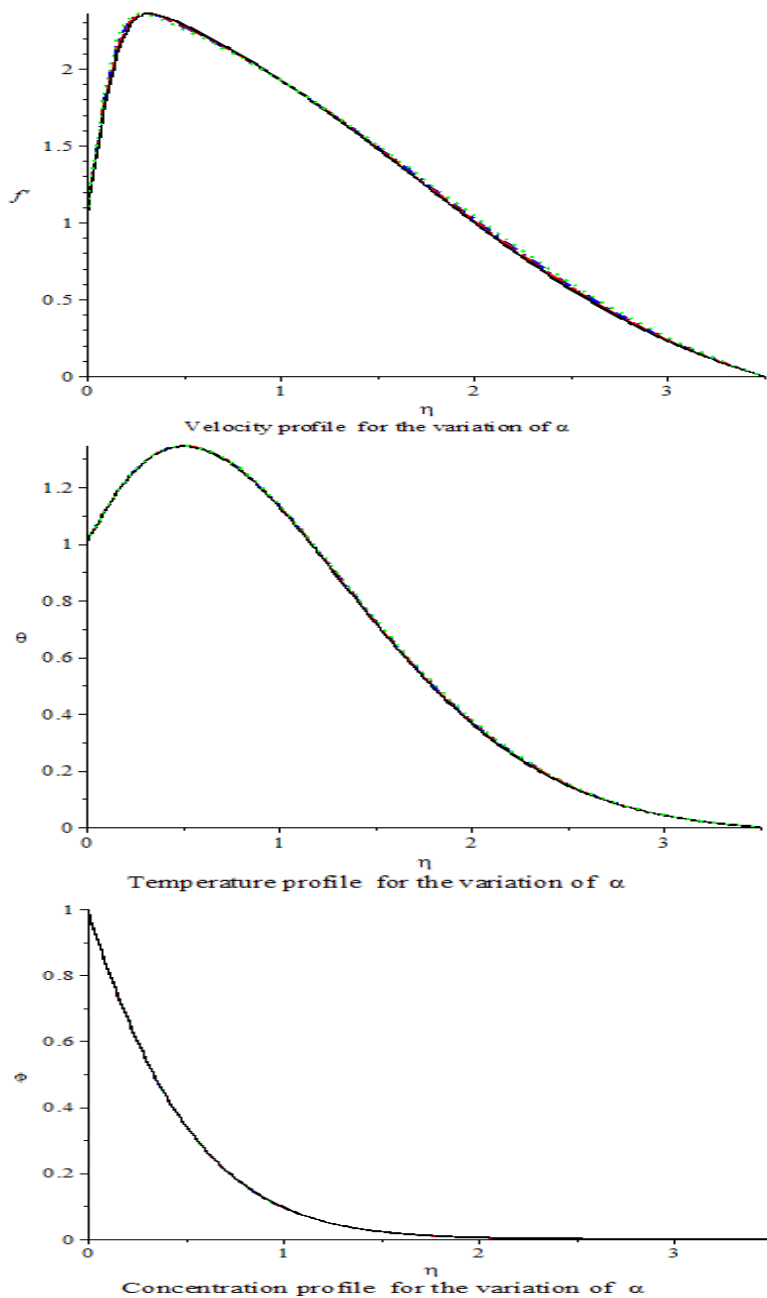


Figure 7: α effect on velocity, temperature and concentration profiles

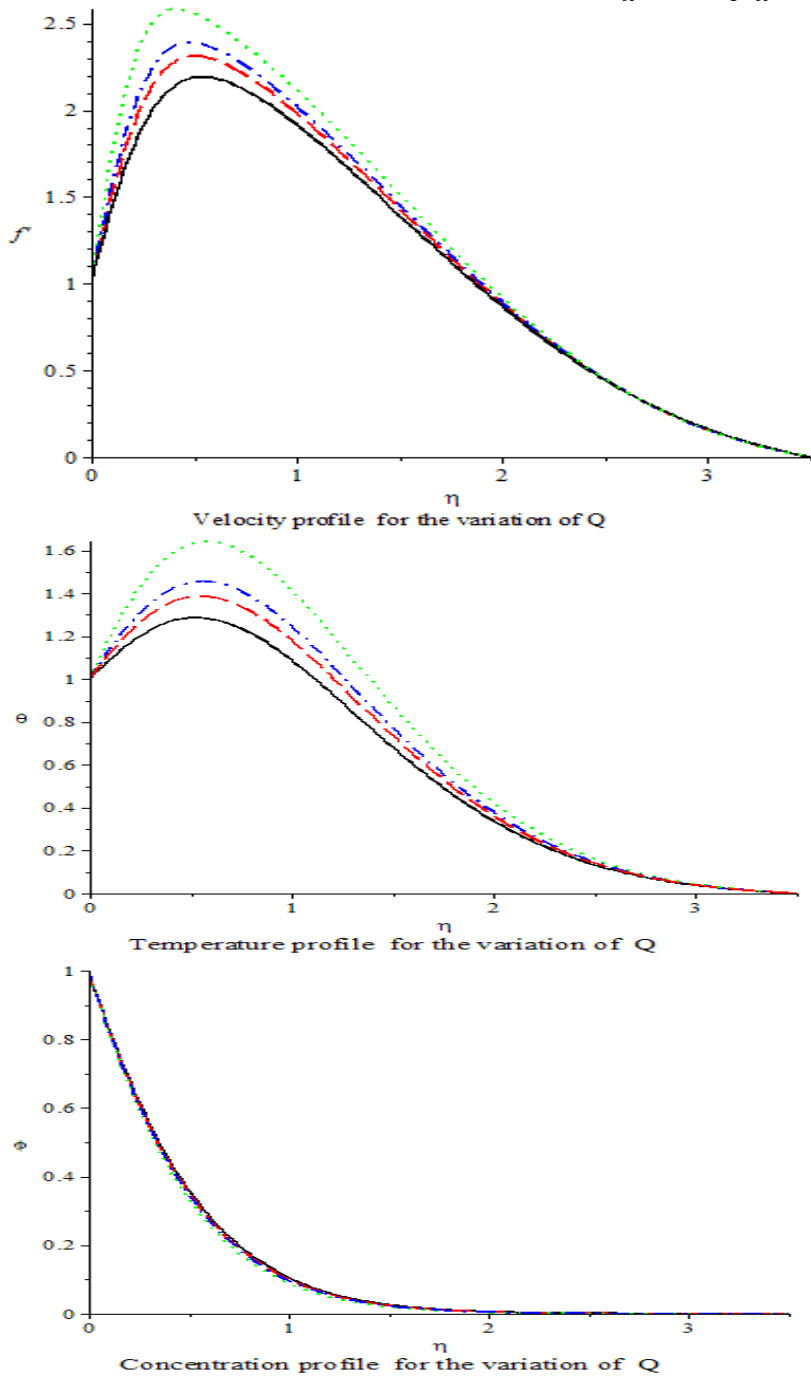


Figure 8: Q effect on velocity, temperature and concentration profiles

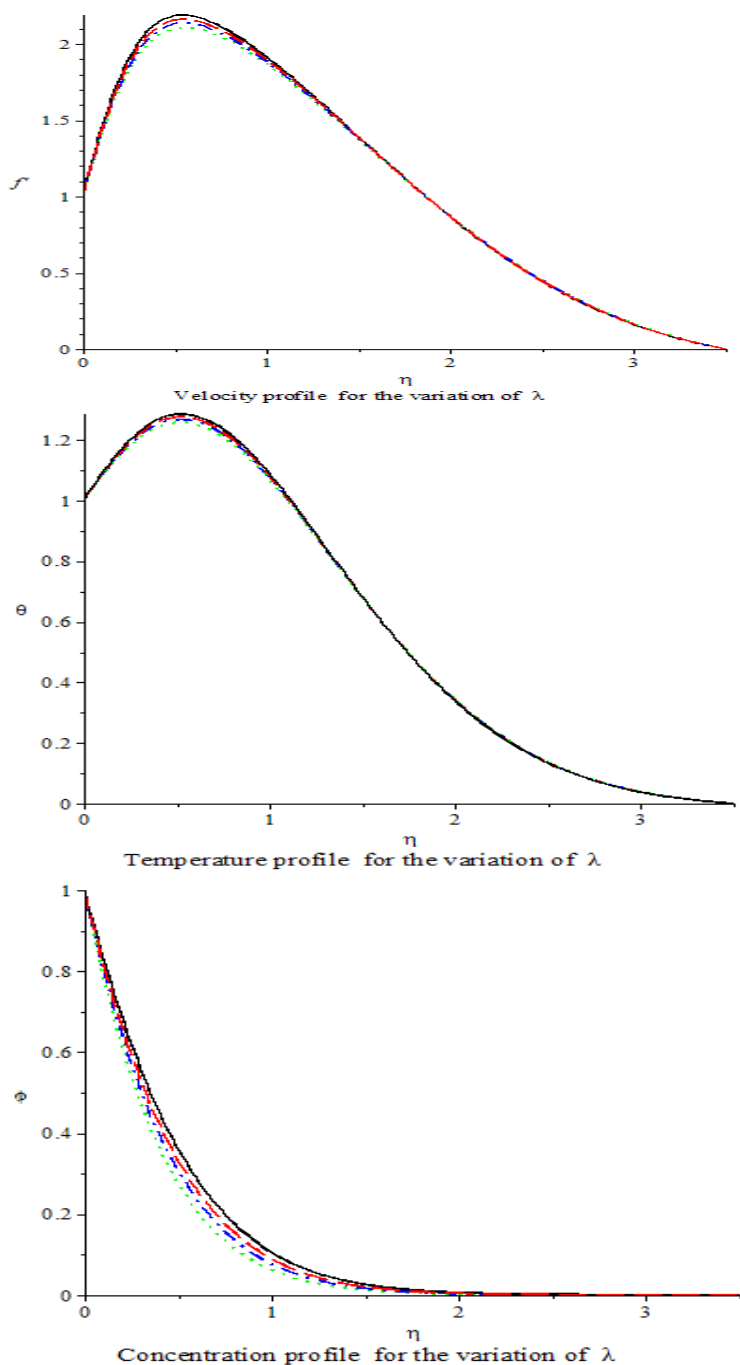


Figure 9: λ effect on velocity, temperature and concentration profiles

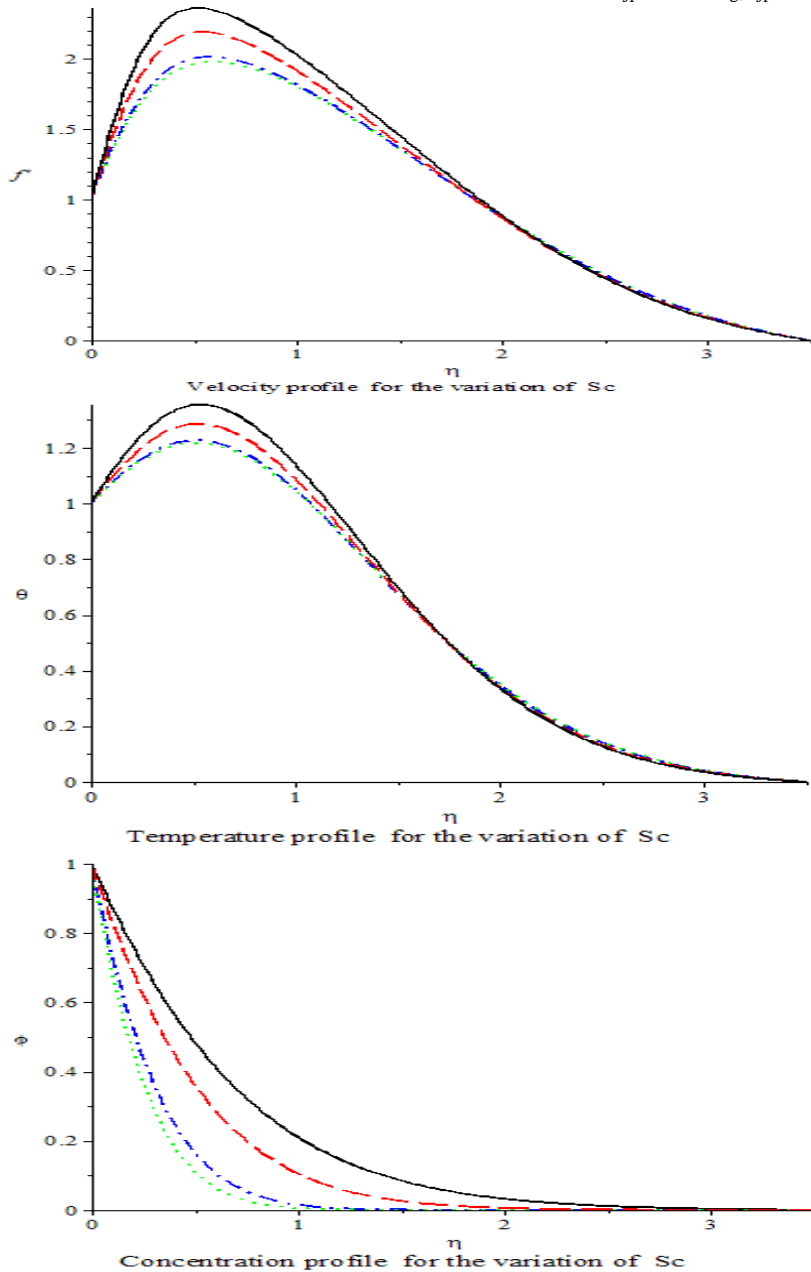


Figure 10 Sc . effect on velocity, temperature and concentration profiles

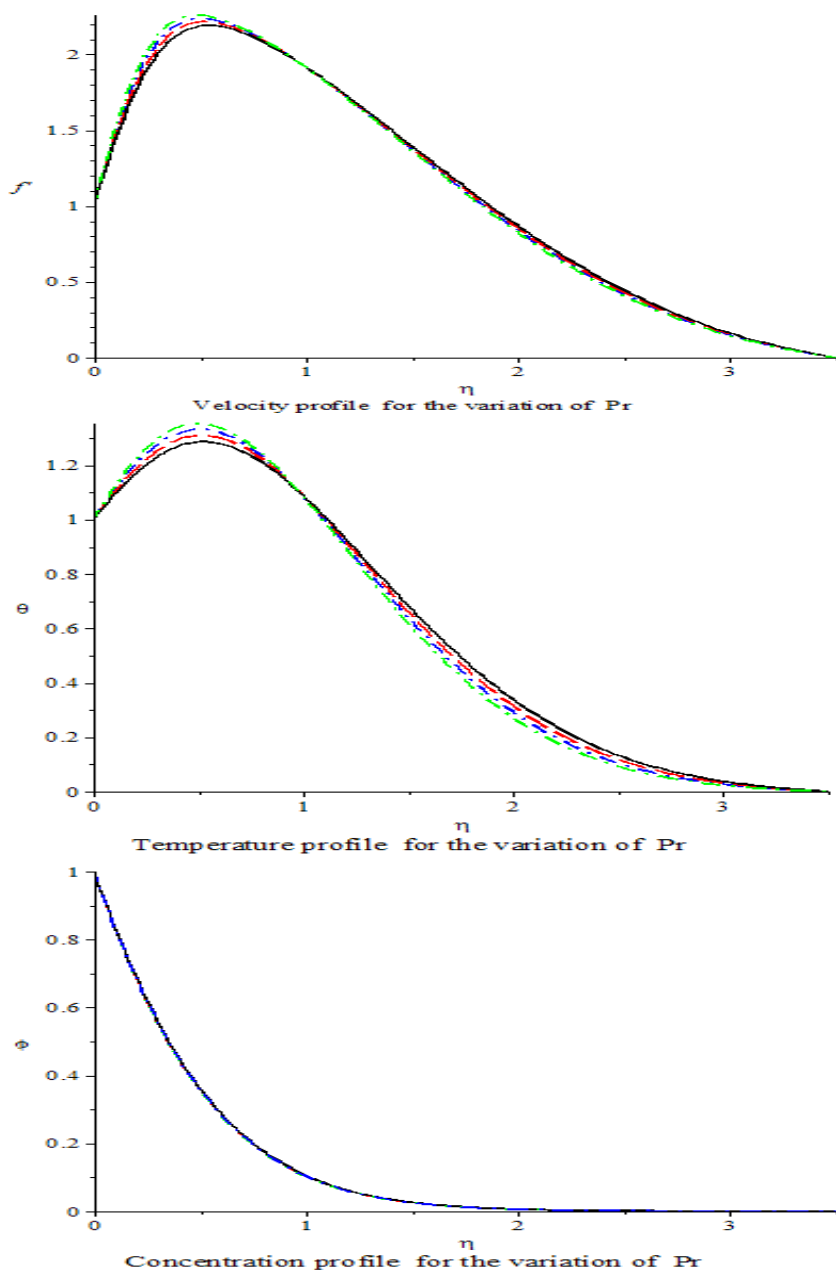


Figure 11: Pr. effect on velocity, temperature and concentration profiles

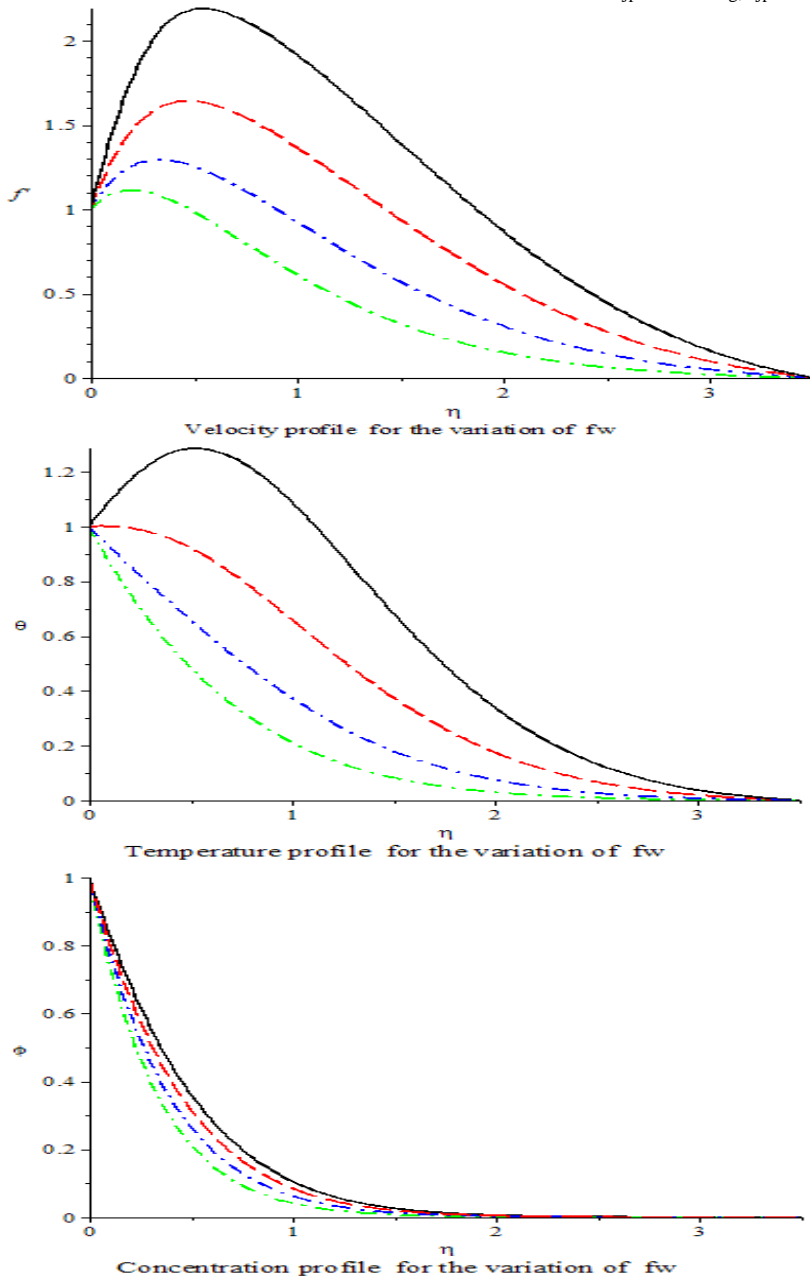


Figure 12: fw effect on velocity, temperature and concentration profiles

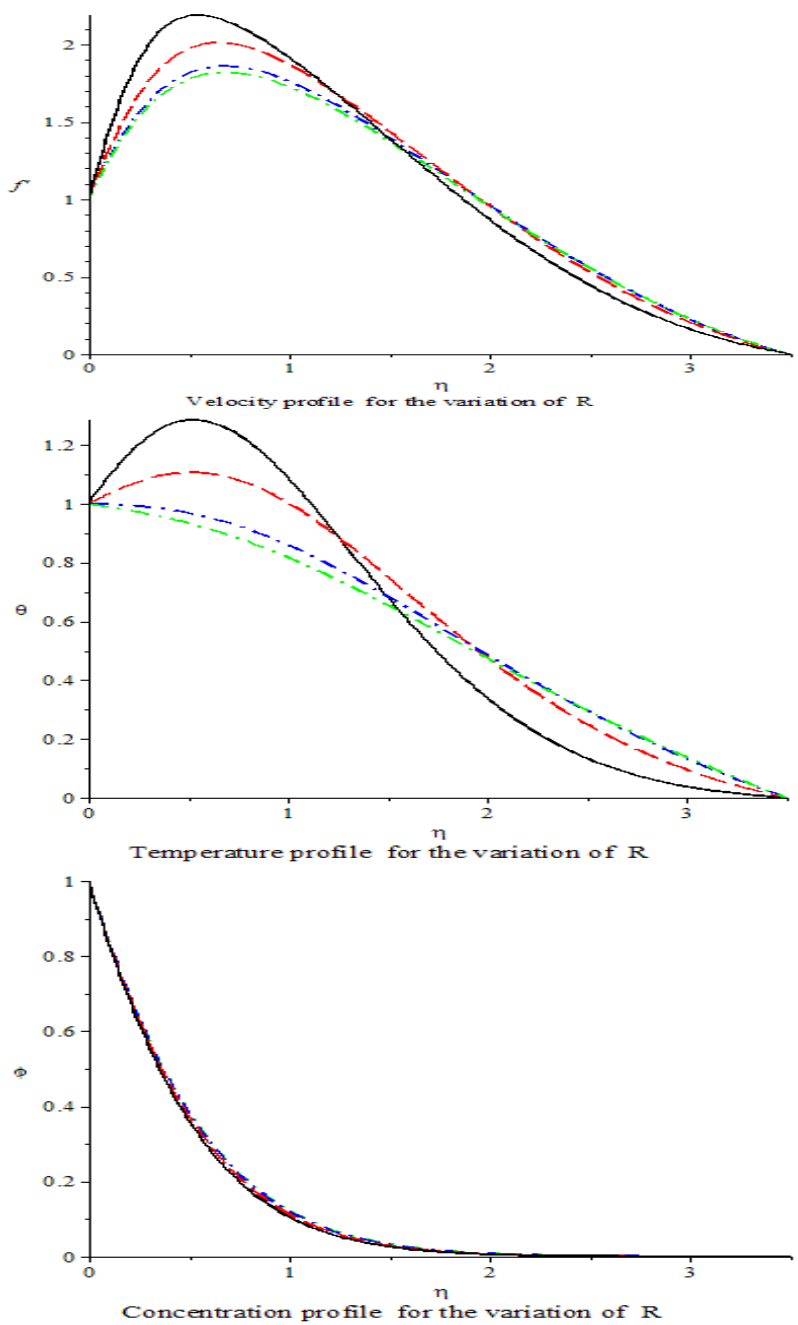


Figure 13: R effect on velocity, temperature and concentration profiles

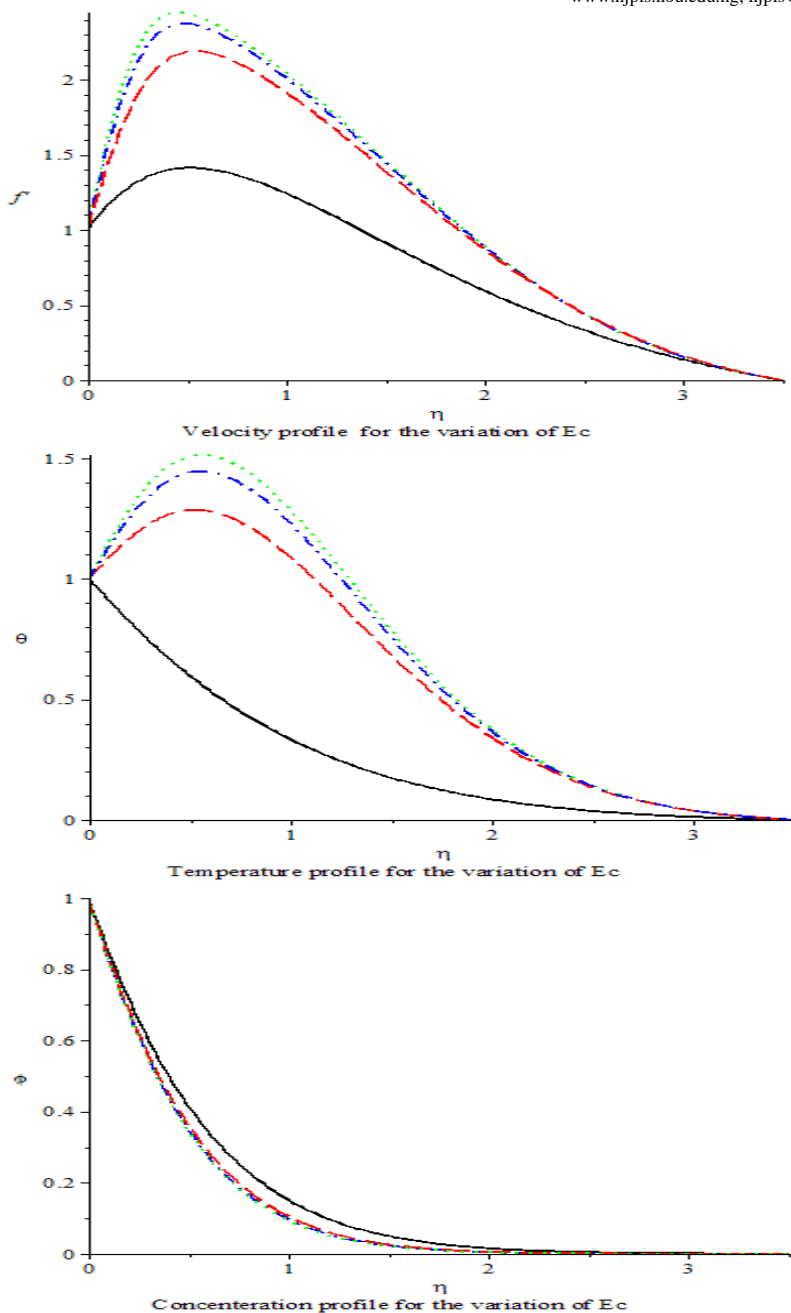


Figure 14: Ec . effect on velocity, temperature and concentration profiles

REFERENCES

- Amoo, S. A. Makar, M. and Amoo, A. O. (2017). Magnetohydrodynamics flow of heat and mass transfer embedded in thermally stratified media over exponentially-stretching sheet. At 5th Faculty of Science Conference, Lagos State University, Ojo, Lagos. 10th -14th October, 2017. Page 6.
- Amoo, S. A. and Idowu, A. S. (2017) Thermal radiation effects on heat and mass transfer of MHD flow in porous media over an exponentially stretching surface. *FUW Trends in Science and Technology Journal* 2 (1A): 33-41.
- Anderson, H. I. (2002). Slip flow past a stretching surface, *Acta Mech.*, 158, 121-125.
- Bhattacharyya, K. and Layek, G. C. (2010). Chemically reactive solute distribution in MHD boundary layer flow over a permeable stretching sheet with suction or blowing. *Chemical Eng. Commun.*, 197, 1527-1540.
- Disu, A. B. and Dada, M. S. Reynold's model viscosity on radiative MHD flow in a porous medium between two vertical wavy walls. *Journal of Taibah University for Science* 11 (4), 548 – 565.
- Devi, R. L. V. R, Neeraja, A and Reddy, N. B. (2015). Radiation effect on MHD slip flow past a stretching sheet with variable viscosity and heat source/sink. *International Journal of Scientific and innovative Mathematics Research*, 3(5): 8-17.
- Ibrahim, S. M. and Sunnetha, K. (2015). Effect of heat generation and thermal radiation on MHD flow near a stagnation point on a linear stretching sheet in porous medium and presence of variable thermal conductivity and mass transfer. *Journal of Computational and*

- Applied Research in Mechanical Engineering* 4(2), 133-144.
- Mukhopadhyay, S. and Gorla, R. S. K. (2012). Effects of partial slip on boundary layer flow past a permeable exponential stretching sheet in presence of thermal radiation. *Heat and Mass Transfer* 48, 1773–1781.
- Mukhopadhyay, S. (2013). Slip effects on MHD boundary layer flow over an exponentially stretching sheet with suction/blowing and thermal radiation. *Ain Shams Eng. Journal* 4(1), 485-491
- Sajid, M. and Hayat, T (2008). Influence of thermal radiation on the boundary layer flow due to an exponentially stretching sheet, *Int. Commun. Heat Mass Transfer* 35, 347-356.
- Shekhar, K. V. C. (2014). Boundary layer Phenomena of MHD flow and Heat transfer over an exponentially stretching sheet embedded in a thermally stratified medium. *International Journal of Science, Engineering and Technology Research*, 3(10), 2715-2721.

